


Depth Control of a Bioinspired Robotic Dolphin Based on Sliding-Mode Fuzzy Control Method

Junzhi Yu , Senior Member, IEEE, Jincun Liu, Zhengxing Wu , and Hao Fang 

Abstract—This paper presents a hybrid controller that combines sliding-mode control (SMC) with a fuzzy strategy to regulate the vertical displacement of a bioinspired robotic dolphin. The structure of the robot and a simplified mathematical model for depth control are described. An SMC based on the line-of-sight guidance law and the sliding-mode observer is developed to overcome systematic uncertainties and environmental disturbances. The Lyapunov stability theory is utilized to analyze the stability and convergence properties of the closed-loop system. Depth control in the physical robot is realized by utilizing a fuzzy logic controller, which is represented as the mapping of the input propulsion forces/moments and output control parameters. Numerical and experimental results show that the proposed control strategy successfully steers the robot toward and along the desired depth.

Index Terms—Bioinspired robotic dolphin, depth control, fuzzy logic, sliding-mode control (SMC).

I. INTRODUCTION

IN NATURE, aquatic animals have the characteristic of vertical distribution, which is of great significance to reduce spatial competition. Depth control is important to achieve the

Manuscript received April 25, 2017; revised July 13, 2017; accepted August 13, 2017. Date of publication August 29, 2017; date of current version December 15, 2017. This work was supported in part by the National Natural Science Foundation of China under Grant 61633020, Grant 61633017, Grant 61603388, and Grant 61633004, in part by the Beijing Natural Science Foundation under Grant 4164103 and Grant 4161002, in part by the National Defense Science and Technology Innovation Fund of the Chinese Academy of Sciences under Grant CXJJ-16M110, and in part by the Beijing Advanced Innovation Center for Intelligent Robots and Systems under Grant 2016IRS02. (Corresponding author: Zhengxing Wu.)

J. Yu is with the State Key Laboratory of Management and Control for Complex Systems, Institute of Automation, Chinese Academy of Sciences, Beijing 100190, China, and also with the Beijing Advanced Innovation Center for Intelligent Robots and Systems, Beijing Institute of Technology, Beijing 100081, China (e-mail: junzhi.yu@ia.ac.cn).

J. Liu is with the State Key Laboratory of Management and Control for Complex Systems, Institute of Automation, Chinese Academy of Sciences, Beijing 100190, China, and also with the University of Chinese Academy of Sciences, Beijing 100049, China (e-mail: liujincun2015@ia.ac.cn).

Z. Wu is with the State Key Laboratory of Management and Control for Complex Systems, Institute of Automation, Chinese Academy of Sciences, Beijing 100190, China (e-mail: zhengxing.wu@ia.ac.cn).

H. Fang is with the Beijing Advanced Innovation Center for Intelligent Robots and Systems, Beijing Institute of Technology, Beijing 100081, China (e-mail: fangh@bit.edu.cn).

Color versions of one or more of the figures in this paper are available online at <http://ieeexplore.ieee.org>.

Digital Object Identifier 10.1109/TIE.2017.2745451

vertical distribution of fish. After the long-term natural selection, nature has evolved many novel and effective depth control mechanisms suitable for a variety of environments [1]. For instance, pectoral fins are of vital importance for some aquatic animals, such as sharks and dolphins, to maintain balance and help them swim up/down to a certain extent. Other species have a closed swim bladder that controls the specific gravity of the fish, thus allowing it to remain at certain depths without using additional energy. Furthermore, fish/whales have developed amazing swimming skills with high speed, high maneuverability, and striking efficiency that are far better than conventional propeller-driven underwater vehicles. There is a growing interest in the development of underwater robots that propel and maneuver themselves like a real fish [2]–[5].

In the context of bioinspired underwater vehicles, depth control is also an important issue to fulfill a great variety of practical applications, such as ocean exploration, seabed mapping, water monitoring, underwater pipelines tracking, etc. Depth control has witnessed a growing number of studies in the areas of mechanical design and robust control. For example, Zhou *et al.* developed a heave locomotion robotic fish that included a barycenter adjuster to change the center of gravity by moving an inside weight, and they presented a controller with deformation compensation to adjust the turning angle of the barycenter-adjuster's servomotor on the basis of the depth feedback. Their experimental results showed that the average error and variance were 1.8812 cm and 4.0933, respectively [6]. Shen *et al.* designed a robotic dolphin based on a gravity adjusting unit and adopted a fuzzy PID controller to realize the depth control; the controller had a small average error rate (i.e., the average error range was ± 5 cm) and good unbiasedness [7]. Niu *et al.* built a robotic fish that mimics the cownose ray and employed a fuzzy logic method to adjust the rotation angles of the horizontal tail to achieve the automatic depth control of the robotic fish [8]. Wang *et al.* proposed a new type of bioinspired robot with undulatory fins inspired by cuttlefish and developed a hybrid control strategy that combined active disturbance rejection control with a fuzzy control to achieve the closed-loop depth control [9]. Fuzzy and self-tuning PID controllers (fuzzy-PID) were addressed by Hoang and Vo to control the rotation angle of the pectoral fins in order to make the robotic fish swim toward the desired depth [10]. As bioinspired robots, robotic dolphins that propel and maneuver similar to real dolphins and have characteristics such as high speed, energy economy, enhanced maneuverability, and reduced detection have attracted increasing attention [11], [12].

Therefore, it is necessary to design a robotic dolphin that can mimic the depth control and diving/ascending motions of a real dolphin.

Efforts to design robotic dolphins have led to intense interest in the development of the so-called robust control methods, such as PID [13], backstepping [14], and fuzzy logic [15], to solve the problem of complicated hydrodynamics and parametric uncertainties associated with changing aquatic environments. The PID controller is easy to implement and is still widely used. However, it is difficult to acquire accurate parameters, and therefore, the accuracy of its control cannot be assured. The disadvantage of fuzzy logic is that the controller's performance is affected by fuzzy rules that depend on the experience of the operators [16]. Therefore, fuzzy logic cannot guarantee the stability and robustness of the control system [17]. In most existing backstepping-based techniques, there would be a great velocity that the robot could not reach, in practice, when there existed a large error between the robot's real point and the reference point [16].

In contrast with the above-mentioned methods, sliding-mode control (SMC) has been successfully employed in depth control for autonomous underwater vehicles (AUVs) owing to its insensitivity to model imprecision, parametric uncertainty, and external disturbances [18]–[20]. The major drawback of the conventional sliding-mode controller is the chattering effect caused by the switching inputs of SMC. In addition, it is currently impossible to transform the dynamical model into a standard form. In other words, it is difficult to steer underwater vehicles directly by SMC. In order to overcome these problems, the fuzzy logic method uses linguistic variables as inputs and generates a particular crisp value as output, which has been combined with SMC to approximate the nonlinear unknown dynamics of AUVs [21]. Yu *et al.* introduced a fuzzy sliding-mode controller to achieve diving/surfacing and make the robotic fish remain at the desired depth. The inputs of the fuzzy controller were the sliding-mode surfaces and the output was the derivative of the pectoral angle. The measured steady-state mean depth error was 1.56 cm, whereas the variance was 7.38 [22]. Lakhekar and Saundarmal presented an adaptive fuzzy sliding-mode controller of depth control. Fuzzy logic was used to enhance the tracking performance by adapting an input and output parameter as slope of sliding surface and hitting control gain of fuzzy inference engine [23]. Pezeshki *et al.* applied an adaptive fuzzy SMC scheme to cope with a position tracking problem. Fuzzy logic systems were used to update the slope of the sliding surface, hit the control gain of the sliding-mode method, and estimate the uncertainty parameters online [24]. It is worth noting that owing to the imprecise mathematical model and complicated aquatic environment, most of the literature focuses on the elimination of the chattering effect. However, the assignment of propulsion forces/moments is rarely involved.

The main objective of this paper is to offer a robotic dolphin, a vertical depth control solution, that is a combination of SMC and fuzzy control law. The main contributions can be summarized as follows.

- 1) The mechanical design and dynamic model of the robotic dolphin are built to describe the diving/ascending

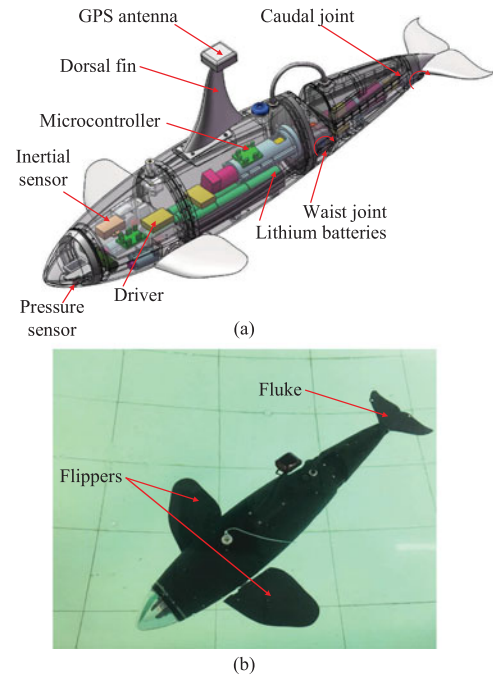


Fig. 1. Illustrations of the mechanical structure of the robotic dolphin. (a) Conceptual design. (b) Robotic prototype.

motion, allowing a comprehensive estimation of depth control.

- 2) Considering the uncertain parameters and unmeasurable swimming velocity of the robotic dolphin, a sliding-mode controller is developed on the basis of a line-of-sight (LOS) guidance and a sliding-mode observer (SMO).
- 3) Based on the SMC, the relationship between propulsion forces/moments and the parameters of diving/ascending motion is explored by a fuzzy parameter mapping method.

The remainder of this paper is structured as follows. The overall description of the mechanical design and a simplified dynamical model for depth control is provided in Section II. Section III gives the detailed analysis of the sliding-mode fuzzy controller based on the LOS and SMO. Aquatic experiments on the physical robot and related discussion are offered in Section IV. Finally, Section V concludes this paper with an outline of future work.

II. MECHANICAL DESIGN AND DYNAMIC MODELING

A. Mechanical Design

In nature, a pair of flippers is endowed with the ability of feathering motion to realize diving/ascending motion for dolphins. The mechanical design was inspired by this fact and was also based on our previous work [11], [12], [25]–[27]. The conceptual design and a prototype of the robot are depicted in Fig. 1. In particular, a well-streamlined shape that is modeled after killer whales is considered to reduce the hydrodynamic drag effect when it swims at a speed. The total length and mass are 0.84 m and 8.8 kg, respectively. The corresponding specifications of the developed robotic dolphin are provided in Table I. The robotic

TABLE I

TECHNICAL PARAMETERS OF THE DEVELOPED ROBOTIC DOLPHIN

Items	Characteristics
Size ($L \times W \times H$)	$\sim 839.71 \times 383.56 \times 334.57 \text{ mm}^3$
Total mass	$\sim 8.8 \text{ kg}$
Number of the body joints	4
Drive mode	DC motors, digital servomotors
On-board sensors	Inertial sensor, pressure sensor, GPS
Power supply	DC 24 V
Operation time	$\sim 3 \text{ h}$
Controller	STM32F407 (ARM based)

dolphin consists of a waist joint and a caudal joint, which are coordinated to implement symmetrical dorsoventral oscillations and produce large thrust forces. A pair of independent degree-of-freedom (DOF) mechanical flippers is employed to achieve diving and surfacing, in which the magnitude and direction can be adjusted by modifying the flippers deflection. In order to solve the waterproofing issues, the fluororubber O-ring and the dynamic seal unit consisting of two Glyd rings are utilized for static and dynamic seal, respectively. The fluororubber O-ring is employed for static seal between these cabins of the robot. As for the dynamic seal of the output shafts, a special dynamic seal unit comprising two Glyd rings is designed. The Glyd ring is a typical dynamic seal product, comprising a dynamic ring made of polytetrafluoroethylene for high wear resistance and a rubber O-ring for elastic compensation. The maximum work pressure that Glyd ring bears is up to 30 MPa. In our pressurization tests, the dynamic seals can operate normally below 150 m [28].

In addition, the robotic dolphin is equipped with diverse on-board sensors that enable it to achieve stable movements. An absolute pressure sensor (CYG-505ALLF) fixed on the bottom surface offers depth data. Because the original output is only at millivolt level, which is too low to be directly measured by microcontroller unit (MCU), a voltage amplifier for signal processing is developed. Thanks to the custom-built electronic circuit, these signals can be amplified to a linear region. The accuracy can thereby be guaranteed. On the other hand, an average filter is adopted to eliminate noise and guarantee precision. An inertial sensor is utilized to offer attitude and heading direction with its x -axis being along the robot's longitudinal axis.

B. Kinematics and Dynamics

In order to explicitly describe the motion of the robotic dolphin in 6 DOFs, as shown in Fig. 2, it is convenient to define two coordinates, i.e., body-fixed reference frame $O_b\text{-}xyz$ and earth-fixed reference frame $O_g\text{-}xyz$. For the robot moving in 6 DOFs, the general motion of the robot can be described intuitively. The position vector $\eta_1 = [x, y, z]^T$ and orientation vector $\eta_2 = [\phi, \theta, \psi]^T$ of the robot are denoted in the earth-fixed frame, the linear velocity vector $v_1 = [u, v, w]^T$ and angular velocity vector $v_2 = [p, q, r]^T$ are described with coordinates in the body-fixed frame.

The first time derivative of the position vector and orientation vector is related to the linear velocity vector and angular velocity

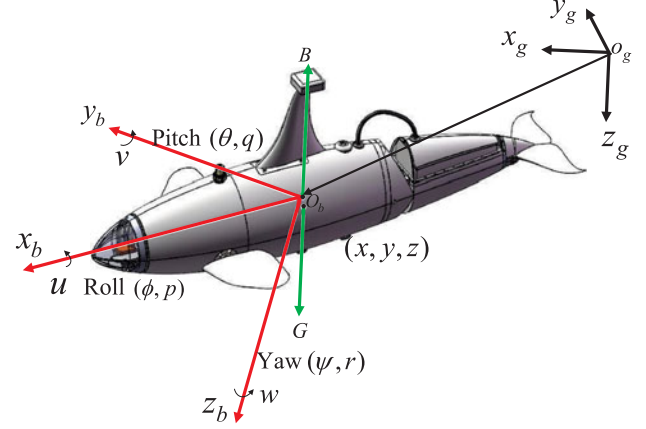


Fig. 2. Body-fixed and earth-fixed reference frames of the robotic dolphin.

vector through the following transformation:

$$\begin{aligned}\dot{\eta}_1 &= J_1 v_1 \\ \dot{\eta}_2 &= J_2 v_2\end{aligned}\quad (1)$$

where J_1 and J_2 are the transformation matrices that are related to the functions of the Euler angles roll (ϕ), pitch (θ), and yaw (ψ). In general, the hydrodynamic model of the robotic dolphin neglecting the nonlinear coupling can be written as

$$M\dot{v} = -C(v)v - D(v)v - g(\eta) + \tau + \tau_E \quad (2)$$

where $v = [v_1, v_2]^T$, the matrices M denotes the rigid body system inertia including added mass, $C(v)$ is the matrix of Coriolis and Centripetal terms including added mass, and the damping matrix is defined as $D(v)$. $g(\eta)$ denotes the restoring forces and moments vector in the body-fixed coordinate system. τ is a generalized vector of external forces and moments, and τ_E represents the environmental disturbances.

With respect to the vertical motion of the robotic dolphin, the following physically based assumptions can be made.

- 1) The motions of roll and yaw are ignored, i.e., $y = 0$, $v = 0$, $p = 0$, $r = 0$, $\phi = 0$, and $\psi = 0$.
- 2) The robotic dolphin is neutrally buoyant, it means that the gravitational force (G) is equal to buoyant force (B) so that gravity and buoyancy cancel each other out. Furthermore, the center of buoyancy (Z_b) and the center of the gravity (Z_g) are located in the vertical plane.
- 3) The hydrodynamic damping coefficients of the robot are time varying but assumed to be known and noncoupled, so the diagonal structure of $D(v)$ with only linearized damping forces/moments ($-X_u$, $-Z_w$, and $-M_q$) and quadratic damping terms ($-X_{u|u}|u|$, $-Z_{w|w}|w|$, and $-M_{q|q}|q|$) on the diagonal.

Based on the above-mentioned assumptions, the matrices M , $C(v)$, $D(v)$, $g(\eta)$, v , τ , and τ_E are supposed to have the

following structure:

$$\begin{aligned}
 M &= \begin{bmatrix} m_{11} & 0 & 0 \\ 0 & m_{22} & 0 \\ 0 & 0 & m_{33} \end{bmatrix} \\
 C(v) &= \begin{bmatrix} 0 & 0 & m_{22}w \\ 0 & 0 & -m_{11}u \\ -m_{22}w & m_{11}u & 0 \end{bmatrix} \\
 D(v) &= \begin{bmatrix} d_{11} & 0 & 0 \\ 0 & d_{22} & 0 \\ 0 & 0 & d_{33} \end{bmatrix} \\
 g(\eta) &= \begin{bmatrix} 0 \\ 0 \\ -(Z_b B - Z_g G) \sin \theta \end{bmatrix} \\
 &= \begin{bmatrix} 0 \\ 0 \\ -\overline{BG_z} B \sin \theta \end{bmatrix} \\
 v &= [u \quad w \quad q]^T \\
 \tau &= [X \quad 0 \quad M]^T \\
 \tau E &= [\tau_{uE} \quad \tau_{wE} \quad \tau_{qE}]^T
 \end{aligned} \quad (3)$$

where $m_{11} = m - X_{\dot{u}}$, $m_{22} = m - Z_{\dot{w}}$, $m_{33} = I_y - M_{\dot{q}}$, $d_{11} = -X_u - X_{u|u}|u|$, $d_{22} = -Z_w - Z_{w|w}|w|$, and $d_{33} = -M_q - M_{q|q}|q|$. m is the mass of the robotic dolphin. The $X_{\dot{u}}$, $Z_{\dot{w}}$, and $M_{\dot{q}}$ are the added mass in the x -, z -, and q -direction, respectively. X and M represent the propulsion forces and pitch moments, respectively. $\overline{BG_z}$ means the distance from barycenter to the center of buoyancy. I_y is the moment of inertia about $O_b Y_b$.

According to (1)–(3), the dynamic model of the robotic dolphin is simplified as

1) kinematics

$$\begin{aligned}
 \dot{x} &= u \cos \theta + w \sin \theta \\
 \dot{z} &= -u \sin \theta + w \cos \theta \\
 \dot{\theta} &= q
 \end{aligned} \quad (4)$$

2) kinetics

$$\begin{aligned}
 \dot{u} &= -\frac{m_{22}}{m_{11}} w q - \frac{d_{11}}{m_{11}} u + \frac{X}{m_{11}} + \frac{\tau_{uE}}{m_{11}} \\
 \dot{w} &= \frac{m_{11}}{m_{22}} u q - \frac{d_{22}}{m_{22}} w + \frac{\tau_{wE}}{m_{22}} \\
 \dot{q} &= \frac{m_{22} - m_{11}}{m_{33}} w u - \frac{d_{33}}{m_{33}} q - \frac{\overline{BG_z} B \sin \theta}{m_{33}} \\
 &\quad + \frac{M}{m_{33}} + \frac{\tau_{qE}}{m_{33}}.
 \end{aligned} \quad (5)$$

III. DEPTH CONTROL OF THE ROBOTIC DOLPHIN

A. LOS Diving Laws

The LOS guidance method that maps the desired tracking points to the targets is an important precondition to steer the

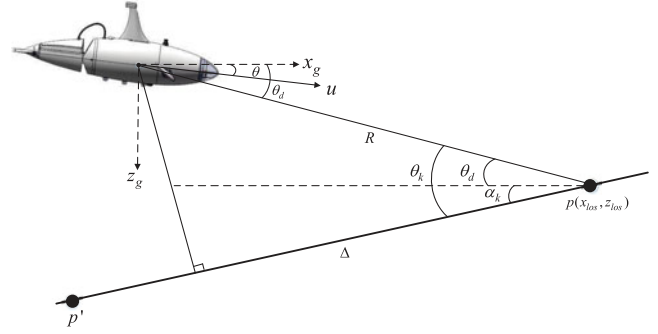


Fig. 3. Schematic diagram of the LOS diving laws.

robotic dolphin along a straight-line path [29]. As shown in Fig. 3, consider a circle with a radius larger than zero, whose center is located in the center of gravity of the robot. If the radius is selected to be sufficiently large, the circle will intersect the straight-line at two points, i.e., the foresight point $p(x_{los}, z_{los})$ and the other intersection p' . The enclosure-based strategy for driving z_e to zero is equal to drive the robotic dolphin toward to the desired course angle θ_d .

As for the straight-line path, the path-tangential angle that is denoted by α_k is a constant. For lookahead-based diving, the desired course angle θ_d can be calculated as

$$\theta_k = \theta_d + \alpha_k \quad (6)$$

where θ_k is a velocity-path relative angle, which ensures that the velocity is directed toward a point on the path that is located at a lookahead distance $\Delta > 0$. According to Fig. 3, we have

$$\begin{cases} \theta_k = \arctan(\frac{Z_e}{\Delta}) \\ Z_e^2 + \Delta^2 = R^2. \end{cases} \quad (7)$$

According to the depth control, α_k is defined as zero and (7) becomes

$$\theta_d = \text{atan2}(Z_e, \sqrt{R^2 - Z_e^2}). \quad (8)$$

B. Design of the SMO

The following position tracking errors are defined as

$$\begin{cases} x_e = x - x_d \\ z_e = z - z_d \\ \theta_e = \theta - \theta_d \end{cases} \quad (9)$$

where x_d and z_d are the desired position and depth of the robot, respectively. According to (4), we can get

$$\begin{bmatrix} u \\ w \end{bmatrix} = \begin{bmatrix} \cos \theta & -\sin \theta \\ \sin \theta & \cos \theta \end{bmatrix} \begin{bmatrix} \dot{x} \\ \dot{z} \end{bmatrix}. \quad (10)$$

The tracking error of swimming velocity is defined as $u_e = u - u_d$. Based on (8) and (9), it should be noted that the convergence of u_e and θ_e implies that x_e and z_e converge to zero [30].

It is difficult to obtain the vehicle's speed without Doppler velocity logs. The state observer that needs to be fed with all variables of the internal state of the system is utilized as a solution [31], [32]. In the course of submergence, we estimate

the linear velocity vector on the basis of z_e . An SMO is chosen as

$$\begin{aligned}\dot{\hat{u}} &= -\frac{m_{22}}{m_{11}}wq - \frac{d_{11}}{m_{11}}\hat{u} + \frac{X}{m_{11}} + d_1 - L_1 \tanh(\tilde{z}/\phi) \\ \dot{\hat{z}} &= -\hat{u} \sin(\theta) + w \cos(\theta) - L_2 \tanh(\tilde{z}/\phi) \\ \tilde{z} &= c(\hat{z} - z)\end{aligned}\quad (11)$$

where \hat{z} and \hat{u} are the estimated values of z and u , respectively, and \tilde{z} represents the estimation error. A hyperbolic tangent function with a boundary layer thickness ϕ is chosen to remove chattering and noise.

C. Sliding-Mode Control

Within the framework of SMC methods, the n th-order problems are often transformed into first-order ones. The good performance achieved by this transformation is obtained with high control activity, which may impose limitations on the implementation in certain systems [33]. Owing to the insensitivity of SMC to model mismatches, it is commonly favored as a powerful robust control method for dynamic positioning and motion control [34]. In this section, an SMC algorithm is developed for depth control of the robotic dolphin. In other words, the problem is to design a feedback control law that can drive the output tracking errors to zero. Lyapunov stability criteria are utilized to analyze the closed-loop system stability.

In order to realize the control objective, a first-order exponentially stable surface (S_1) in terms of the swimming velocity tracking error and a sliding surface (S_2) according to the course angle tracking error are chosen by the following equation:

$$S_1 = \lambda_1 \int_0^t u_e(\tau) d\tau + u_e, \quad \lambda_1 > 0 \quad (12)$$

$$S_2 = \lambda_2 \theta_e + \dot{\theta}_e, \quad \lambda_2 > 0 \quad (13)$$

where λ_1 and λ_2 are positive constants that determine the slope of the sliding surfaces. Taking the derivative of (12) and (13) with respect to time, we get

$$\dot{S}_1 = \lambda_1 u_e + \dot{u}_e = \lambda_1 u_e + \dot{u} - \dot{u}_d \quad (14)$$

$$\dot{S}_2 = \lambda_2 (\dot{\theta} - \dot{\theta}_d) + (\ddot{\theta} - \ddot{\theta}_d). \quad (15)$$

Substituting (5) into (14), we have

$$\begin{aligned}\dot{S}_1 &= \frac{1}{m_{11}}(\lambda_1 m_{11} u_e - m_{22} wq - d_{11} u \\ &\quad + X - m_{11} \dot{u}_d)\end{aligned}\quad (16)$$

Based on (4), (5), and (8), (15) can be rewritten as

$$\begin{aligned}\dot{S}_2 &= \lambda_2 (q - \dot{\theta}_d) + \left(\frac{m_{22} - m_{11}}{m_{33}} wu - \frac{d_{33}}{m_{33}} q \right. \\ &\quad \left. - \frac{\overline{BG}_z B \sin \theta}{m_{33}} + \frac{M}{m_{33}} - \ddot{\theta}_d \right).\end{aligned}\quad (17)$$

The process of SMC can be divided into two phases, namely *equivalent term* ($X_{u,eq}$ and $M_{q,eq}$) and *switching term* ($X_{u,sw}$ and $M_{q,sw}$). The equivalent control law can be easily computed

by solving the equation $\dot{S}_1|_{X=X_{u,eq}} = 0$ and $\dot{S}_2|_{M=M_{q,eq}} = 0$ without considering the parameter uncertainty:

$$X_{u,eq} = -\lambda_1 \hat{m}_{11} u_e + \hat{m}_{22} wq + \hat{d}_{11} u + \hat{m}_{11} \dot{u}_d \quad (18)$$

$$\begin{aligned}M_{q,eq} &= \hat{m}_{33} \ddot{\theta}_d + \overline{BG}_z B \sin \theta + \hat{d}_{33} q \\ &\quad + (\hat{m}_{11} - \hat{m}_{22}) wu + \hat{m}_{33} \lambda_2 (\dot{\theta}_d - q)\end{aligned}\quad (19)$$

where “ $\hat{\cdot}$ ” is used to indicate the estimated hydrodynamic coefficients of the robotic dolphin and is defined as

$$\begin{cases} |m_{ii} - \hat{m}_{ii}| \leq M_{ii} \\ |d_{ii} - \hat{d}_{ii}| \leq D_{ii} \\ M_{ii} = 0.05 m_{ii} \\ D_{ii} = 0.05 d_{ii}. \end{cases} \quad (20)$$

The switching law is used to solve the problem of parameter perturbations and disturbances. With consideration of the drawbacks of the equivalent control law such as chattering, a saturation function $\text{sat}(s)$ is introduced to avoid this phenomenon:

$$\text{sat}(s) = \begin{cases} 1 & s > \sigma \\ \frac{s}{\sigma} & |s| \leq \sigma \\ -1 & s < -\sigma \end{cases} \quad (21)$$

where σ is a positive value and indicates the boundary layer thickness. Therefore, the reaching control law can be given as

$$X_{u,sw} = -K_1 \text{sat}(S_1) m_{11} \quad (22)$$

$$M_{q,sw} = -K_2 \text{sat}(S_2) m_{33}. \quad (23)$$

Here, K_1 and K_2 are chosen as

$$K_1 = \lambda_1 M_{11} |u_e| + M_{22} |wq| + D_{11} |u| + m_{11} |\dot{u}_d| + \delta_1 \quad (24)$$

$$\begin{aligned}K_2 &= \lambda_2 M_{33} |\dot{\theta}_d - q| + M_{33} |\ddot{\theta}_d| + D_{33} |q| \\ &\quad + (M_{11} + M_{22}) |wu| + \delta_2\end{aligned}\quad (25)$$

where δ_1 and δ_2 are decimals greater than zero. Finally, the entire propulsion control input and pitch moments can be calculated:

$$X = X_{u,eq} + X_{u,sw} \quad (26)$$

$$M = M_{q,eq} + M_{q,sw}. \quad (27)$$

Proposition: If the SMC laws that are designed by (12) and (26) are applied to the robotic dolphin, the asymptotic stability of velocity tracking is confirmed in finite time.

Proof: Consider the following Lyapunov function:

$$V_1 = \frac{1}{2} m_{11} S_1^2. \quad (28)$$

It is obvious from (28) that $V_1 > 0$ for $S_1 \neq 0$. The time derivative of V_1 can be derived along with (16), (18), (22), (24), and (26):

$$\begin{aligned}\dot{V}_1 &= m_{11} S_1 \dot{S}_1 \\ &= S_1 (\lambda_1 (m_{11} - \hat{m}_{11}) u_e - (m_{22} - \hat{m}_{22}) wq \\ &\quad - (d_{11} - \hat{d}_{11}) u - (m_{11} - \hat{m}_{11}) \dot{u}_d - K_1 \text{sat}(S_1)) \\ &\leq -\delta_1 |S_1| < 0.\end{aligned}\quad (29)$$

Thus, the control input X is proved to satisfy the sliding surface reaching condition (i.e., $S_1 \dot{S}_1 < 0$), the speed tracking

can reach and stay on the manifold $S_1 = 0$ in finite time. Similarly, we can also prove that the course angle tracking error converges to zero, meaning the depth tracking evolves on the manifold $S_2 = 0$ in finite time. Therefore, the whole system is asymptotically stable.

D. Fuzzy Controller

As mentioned above, the external force X and pitch moments M can be obtained through the SMC. However, it is vital to assign the propulsion forces/moments to each joint of the robotic dolphin reasonably, because the depth control of the robotic dolphin is related to inherently highly coupled nonlinear hydrodynamics, imprecise hydrodynamic coefficients, and environmental disturbances. In addition, the relation between pectoral flipper deflection and pitch moments is nonlinear. Therefore, there is no accurate mathematical model to represent the diving/ascending motion of the robotic dolphin.

To solve these challenging problems, fuzzy logic has been applied to deal with an imprecise complex control system. Furthermore, by taking use of fuzzy partition, it can also avoid the chattering problem of the SMC method. In order to simplify the analysis, the depth control system is commonly decomposed into two noninteractive systems, such as diving/ascending subsystem and driving subsystem. As for the diving/ascending subsystem, the inputs are the pitch moment M and the derived change in pitch moment M_e and the output is the pectoral flipper deflection angle φ . As for the driving subsystem, a central pattern generator (CPG) based controller [27], [35] is utilized to achieve dolphin-like swimming. In order to simplify the subsystem, both amplitudes and phase lags of the CPG model are settled. The inputs for the driving subsystem are the propulsion force X and propulsion force rate X_e , the output is the oscillating frequency of waist joint and the caudal joint.

The ranges of the input and output variables are defined as $M \in [-0.2, 0.2]$, $M_e \in [-3, 3]$, $\varphi \in [-50, 50]$, $X \in [0, 1]$, $X_e \in [-3, 3]$, and $f \in [0, 3]$. The triangle and trapezium membership functions are used for input and output variables. The sets for M , M_e , φ , X , X_e , and f are represented as U_M , U_{M_e} , U_φ , U_X , U_{X_e} , and U_f , respectively. The linguistic fuzzy set is defined as {NB, NM, NS, ZO, PS, PM, PB} for U_M , U_{M_e} , U_φ , and U_{X_e} . The fuzzy set for U_X and U_f are defined as {ZO, PS, PM, PB}. The NB, NM, NS, ZO, PS, PM, and PB are abbreviated form of negative big, negative medium, negative small, zero, positive small, positive medium, and positive big, respectively. The rule bases of fuzzy controller for U_φ and U_f are listed in Tables II and III, respectively. Finally, at the stage of defuzzification, the crisp output is given by the method of center of gravity. As for the width of boundary layer, which can be varied by the crisp output variable, the chattering problem of SMC can also be eliminated.

IV. EXPERIMENTAL INVESTIGATION

A series of tests on the actual robot were conducted in an indoor pool with clear water to investigate the effectiveness and the robustness of the proposed sliding-mode fuzzy control (SMFC) method described in Section III. The dimensions of

TABLE II
RULE BASE OF FUZZY CONTROLLER FOR U_φ

U_φ		U_{M_e}						
		NB	NM	NS	ZO	PS	PM	PB
U_M	NB	PM	ZO	NS	NB	NB	NB	PM
	NM	ZO	ZO	NS	NM	NM	NM	ZO
	NS	PS	PS	ZO	NS	NS	NS	NM
	ZO	PB	PM	PS	ZO	NS	NM	NB
	PS	PM	PS	PS	PS	ZO	NS	NS
	PM	ZO	PM	PM	PM	PS	ZO	NS
	PB	PM	PB	PB	PM	PS	ZO	NS

TABLE III
RULE BASE OF FUZZY CONTROLLER FOR U_f

U_f		U_{X_e}						
		NB	NM	NS	ZO	PS	PM	PB
U_X	ZO	PS	PS	ZO	ZO	ZO	PS	PM
	PS	PM	PM	PS	PS	PS	PM	PM
	PM	PB	PM	PM	PM	PM	PM	PB
	PB	PB	PB	PB	PB	PB	PB	PB

TABLE IV
CONTROL PARAMETERS OF THE ROBOTIC DOLPHIN

Parameters	Value	Parameters	Value
m_{11}	10.8 kg	σ	0.2
m_{22}	13.3 kg	λ_1	10
m_{33}	0.6 kg·m ²	λ_2	10
X_u	-1 kg/m	R	2.6 m
Z_w	-50 kg/m	$Z_{w w }$	-10 kg/m
M_q	-50 kg/m	BG_z	0.03 m
$X_{u u }$	-10 kg/m	$M_{q q }$	-5 kg/m
δ_2	0.1	δ_1	0.1

the pool were $5 \times 4 \times 1.2$ m³ ($L \times W \times H$) and a global camera was installed on the ceiling to provide a measurement of the robot position. The robot had color markers attached. The initial states of the robotic dolphin, such as initial depth, pitch angle, and swimming velocity, were set to zero and the reference swimming velocity (u_d) and depth (z_d) were preset as 0.35 m/s and 0.4 m, respectively. During the experiments, the control parameters are summarized in Table IV.

A. Swimming Tests on Depth Control

A contrast experiment was designed to verify the performance of the SMFC method compared to that of a standard PID controller. The relevant parameters of the PID controller were established by a trial-and-error method as 60, 0.07, and 0.2 for k_p , k_i , and k_d , respectively. The comparative result is illustrated in Fig. 4. It indicated that both controllers were able to eliminate depth error rapidly. However, the SMFC controller took about 10.2 s to reach the desired depth, which was faster than the PID controller. Furthermore, after the steady state was attained,

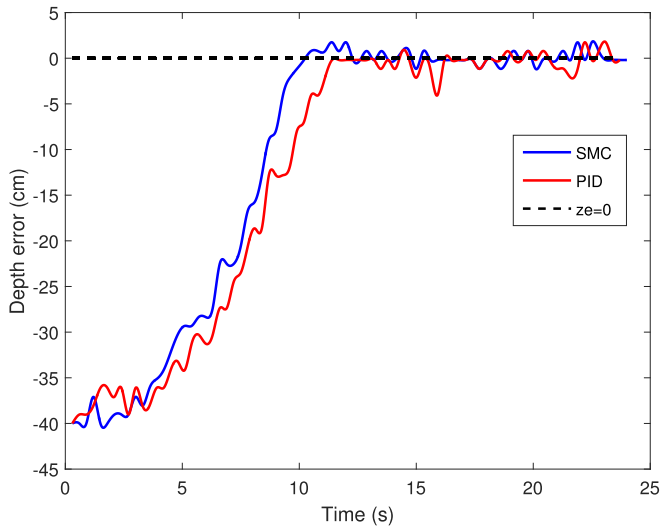


Fig. 4. Depth error during the depth control.

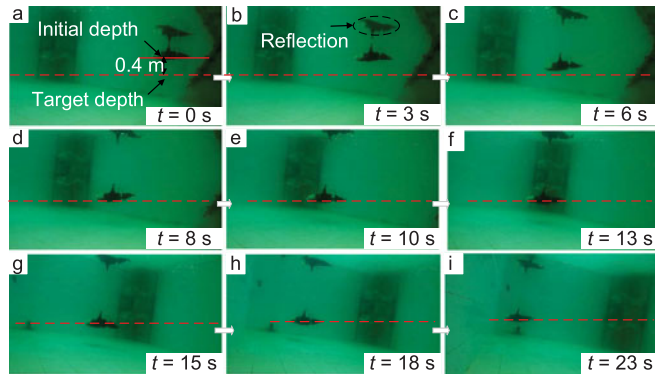
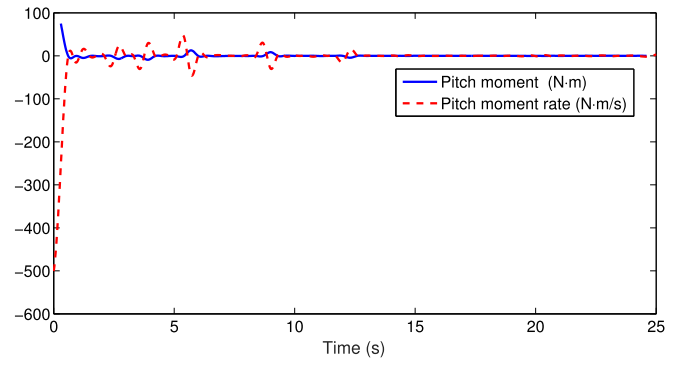


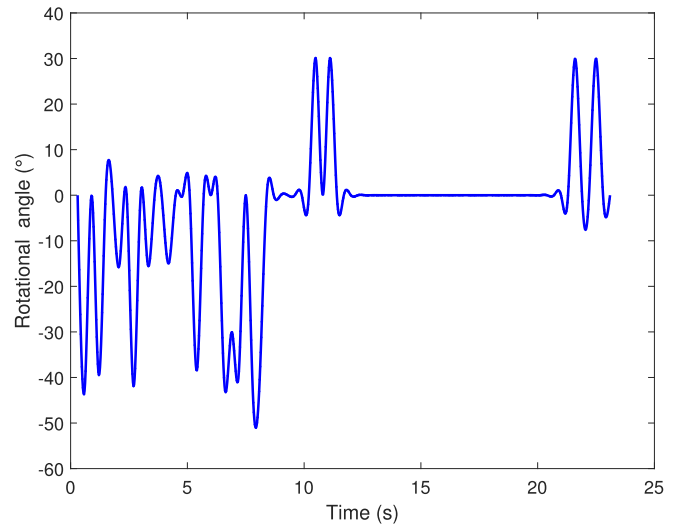
Fig. 5. Snapshot sequences of depth control, which are captured by an underwater camera. The red solid line represents the initial depth of the pressure sensor and the dashed red line indicates the target depth.

depth errors were analyzed. It was calculated that the mean depth errors were 0.18 cm and 0.38 cm for the SMFC and PID controllers, respectively. In addition, as an effective quantitative criterion, the root-mean-square error (RMSE) was used to evaluate the performance of the two controllers. The RMSEs of z_e were 0.60 for the SMFC and 1.27 for the PID controller, which meant that the proposed controller was significantly better than the PID controller.

As for the SMFC, the snapshot sequences of depth control captured by an underwater camera are shown in Fig. 5. This test lasted approximately 24 s. The robot could maintain the desired depth with a period of approximately 10 s corresponding to Fig. 5(a)–(e). In the course of depth control, the robotic dolphin responded sensitively to reduce the depth error by adjusting the rotation angles of the pectoral flippers and by generating a downward/upward force on the flippers. According to (27), the pitch moment M and the pitch moment rate M_e can be calculated. After going through the fuzzification process, the pectoral flipper deflection is demonstrated in Fig. 6. It should be noted that the robotic dolphin must maintain a certain speed to



(a)



(b)

Fig. 6. Control inputs and outputs of the robotic dolphin versus time during the depth control. (a) Pitch moment and pitch moment rate. (b) Rotation angles of the pectoral flippers.

actively adjust the lift. Fig. 7 depicts the corresponding velocity of the robotic dolphin, the reference velocity set as 0.35 m/s, and the velocity estimator obtained by (11); the average swimming speed after the steady state was measured by the global vision system as approximately 0.3 m/s. It reveals that the speed can asymptotically converge to the reference velocity within a reasonable error range.

The inertial sensor installed in the robot's head would still oscillate due to the oscillating motions of the robotic dolphin. Nevertheless, using the median filter, the measured value could effectively eliminate the oscillations. As clearly displayed in Fig. 8, the filtered pitch angle had a good response to the reference angle that was obtained through the LOS diving laws. At the beginning of diving, the pitch angle was oscillating quite strongly; however, it gradually stabilized with a period of approximately 12 s.

B. Anti-Interference Experiment

To ensure a stable depth control performance, an anti-interference experiment was chosen as the test condition. In

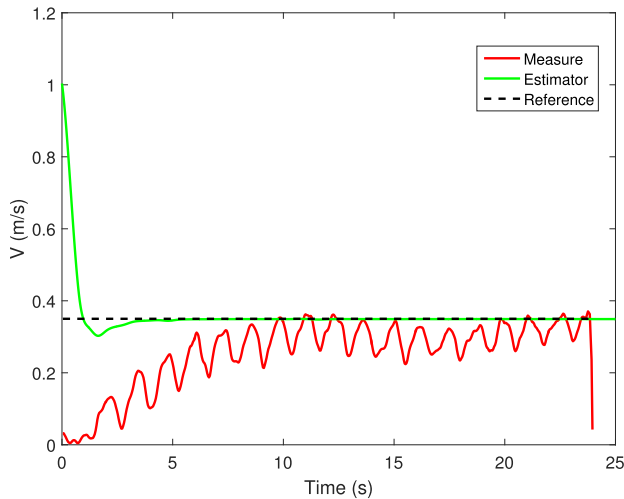


Fig. 7. Swimming velocity as a function of time during depth control.

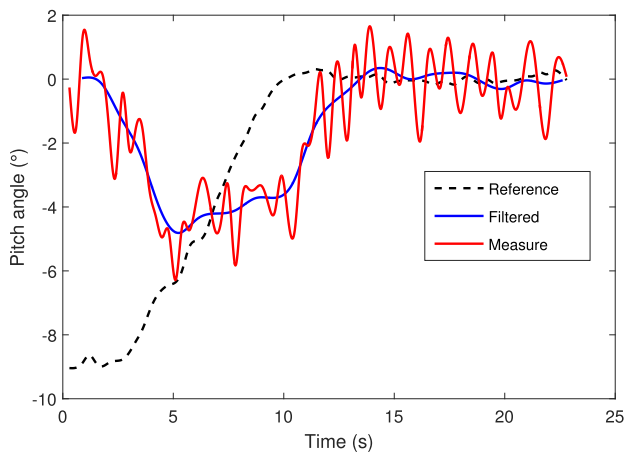


Fig. 8. Time history of pitch attitude during the depth control.

the experiment, the robotic dolphin was first required to dive to a desired depth. As shown in Fig. 9, the robotic dolphin reached the depth of 40 cm after about 8 s, and then kept swimming. In this process, the robotic dolphin had obtained the robustness-related parameters. When $t = 14$ s, an external disturbance was suddenly imposed on the robotic dolphin. Then, the robotic dolphin was forced to sink to a depth of approximately 70 cm. Thanks to the proposed SMFC method, the robotic dolphin ascended back to the reference depth after about 5 s and remained at the target depth. The experiment verified the robustness of the proposed depth control scheme.

C. Depth Switching Experiment

The depth switching was explored to further demonstrate the controller's stability and performance. This experiment was carried out in a larger swimming pool whose dimensions were $18 \times 6 \times 8$ m³. In the experiment, the robotic dolphin was first required to swim at 50 cm underwater. As shown in Fig. 10, the robotic dolphin reached the depth of 50 cm after about 12 s and then kept swimming about 18 s at this level. When $t = 30$ s,

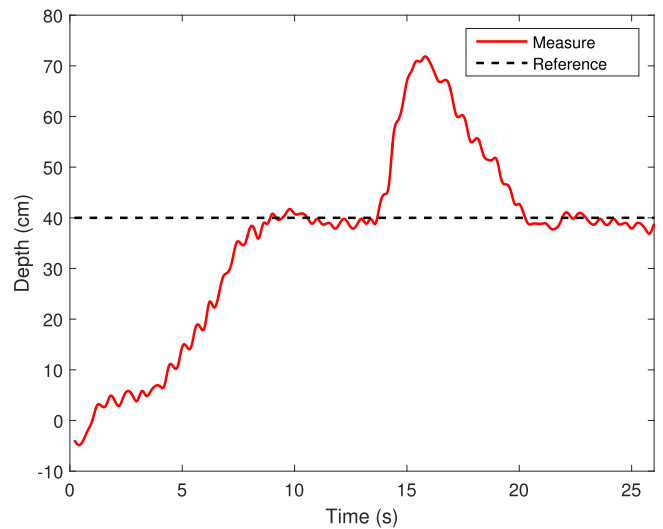


Fig. 9. Result of the anti-interference experiment.

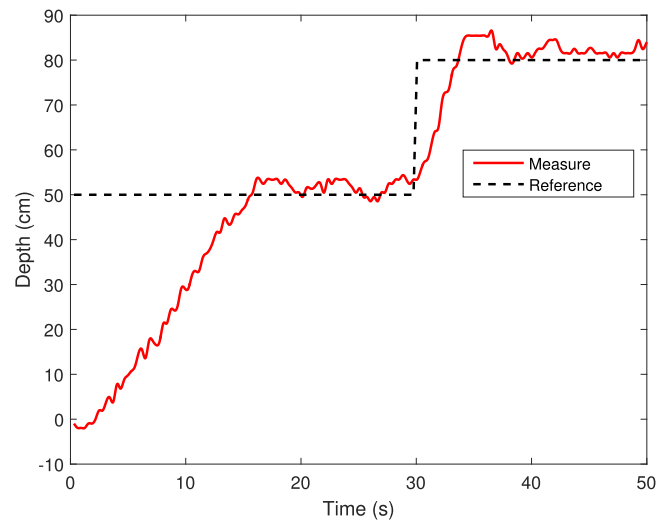


Fig. 10. Result of the depth switching experiment.

the other order of a target depth of 80 cm was set. The robotic dolphin continued to descend and reached the depth of 80 cm after 5 s. During the whole process, the robotic dolphin was able to switch the target depth quickly and timely.

D. Discussion

As a demonstration of coordinated control surfaces, the developed robotic dolphin offers a subtle blend of mechanical structure with functional characteristics. The depth control of the robot not only provides researchers with a unique platform for studying dolphins, but also offers a potential guidance for ocean exploration. We obtain the relationship between propulsion force, moments, pectoral flipper deflection angle, and oscillating frequency, which provides a useful guide to depth control. The designed SMFC contributes to improve the control precision and the antijamming capability. In contrast with Sun's [22] depth control method based on fuzzy SMC, the proposed

control strategy has more accurate fuzzy control input. Compared with the Shen's [7] gravity adjusting unit, it has higher control accuracy by modifying the flippers deflection.

Generally speaking, a fuzzy logic controller cannot guarantee the stability and robustness of the control system. For the hybrid control combining SMC and fuzzy logic, the Lyapunov stability theory has been employed to prove the finite-time stability and convergence properties of the closed-loop system. Furthermore, thanks to the robustness of uncertainty estimation about SMO, the linear velocity can be estimated based on the depth error. Some specific examples, including anti-interference and depth switching experiments, have also demonstrated the finite-time stability and robustness of the proposed control method.

Despite the successful implementation of depth control in the robotic dolphin, there is another issue to be addressed. As illustrated in Fig. 7, an error exists between the theoretical calculation and the practical measurement of the swimming velocity. There are two factors that may cause the error. The first is that the markers are submerged in the pool approximately 0.7 m from the surface, the light refraction from the target to the camera may cause the measuring error. The second is the inaccurate dynamic parameters. Further studies should be carried out to identify an effective mechanism to adjust the dynamic parameters.

V. CONCLUSION AND FUTURE WORK

In this paper, we presented an SMFC law to achieve depth control for a self-propelled robotic dolphin. The up-and-down motion control was achieved by modifying the flippers deflection. In order to realize depth control, the LOS guidance method and SMO were employed to obtain the desired pitch angle and speed estimator, respectively. Based on these data, an SMC was presented and the stability of the system was analytically proved using the Lyapunov stability theory. Furthermore, a fuzzy parameter mapping method was presented to build the nonlinear relationship between the external forces/moments and the control parameters of the robot. Finally, the performance of the SMFC was investigated through experiments. The latest experimental results confirmed the validity of the proposed methods.

The ongoing and future work will focus on the robotic dolphin following a path in a horizontal plane. In addition, a three-dimensional path-following control problem for the robotic dolphin is another ongoing effort.

ACKNOWLEDGMENT

The authors are grateful to the anonymous reviewers and the associate editor for their valuable comments and suggestions on revising this paper.

REFERENCES

- [1] Z. Chen, T. I. Um, and H. Bart-Smith, "Modeling and control of artificial bladder enabled by ionic polymer-metal composite," in *Proc. 2012 Amer. Contr. Conf.*, Montreal, Canada, 2012, pp. 1925–1930.
- [2] S. Zhang, Y. Qian, P. Liao, F. Qin, and J. Yang, "Design and control of an agile robotic fish with integrative biomimetic mechanisms," *IEEE/ASME Trans. Mechatronics*, vol. 21, no. 4, pp. 1846–1857, Aug. 2016.
- [3] W. Wang and G. Xie, "Online high-precision probabilistic localization of robotic fish using visual and inertial cues," *IEEE Trans. Ind. Electron.*, vol. 62, no. 2, pp. 1113–1124, Feb. 2015.
- [4] L. Wen, T. Wang, G. Wu, and J. Liang, "Quantitative thrust efficiency of a self-propulsive robotic fish: Experimental method and hydrodynamic investigation," *IEEE/ASME Trans. Mechatronics*, vol. 18, no. 3, pp. 1027–1038, Jun. 2013.
- [5] C. Zhou and K. H. Low, "Design and locomotion control of a biomimetic underwater vehicle with fin propulsion," *IEEE/ASME Trans. Mechatronics*, vol. 17, no. 1, pp. 25–35, Feb. 2012.
- [6] C. Zhou, Z. Cao, S. Wang, and M. Tan, "Study on the pitching and depth control of biomimetic robot fish," *Acta Automat. Sin.*, vol. 34, no. 9, pp. 1215–1218, 2009.
- [7] F. Shen, Z. Cao, C. Zhou, and D. Xu, "Depth control for robotic dolphin based on fuzzy PID control," *Int. J. Offshore Polar Eng.*, vol. 23, no. 3, pp. 166–252, 2013.
- [8] C. Niu, L. Zhang, S. Bi, and Y. Cai, "Development and depth control of a robotic fish mimicking Cownose ray," in *Proc. IEEE Int. Conf. Robot. Biomimetics*, Guangzhou, China, Dec. 2012, pp. 814–818.
- [9] S. Wang, Y. Wang, Q. Wei, M. Tan, and J. Yu, "A bio-inspired robot with undulatory fins and its control methods," *IEEE/ASME Trans. Mechatronics*, vol. 22, no. 1, pp. 206–216, Feb. 2017.
- [10] K. A. Hoang and T. Q. Vo, "A study on fuzzy based controllers design for depth control of a 3-joint carangiform fish robot," in *Proc. Int. Conf. Control, Autom. Inf. Sci.*, Nha Trang, Vietnam, Nov. 2013, pp. 289–294.
- [11] J. Yu, Z. Su, Z. Wu, and M. Tan, "An integrative control method for bio-inspired dolphin leaping: design and experiments," *IEEE Trans. Ind. Electron.*, vol. 63, no. 5, pp. 3108–3116, May 2016.
- [12] J. Yu, Z. Su, Z. Wu, and M. Tan, "Development of a fast-swimming dolphin robot capable of leaping," *IEEE/ASME Trans. Mechatronics*, vol. 21, no. 5, pp. 2307–2316, Oct. 2016.
- [13] M. H. Khodayari and S. Balochian, "Modeling and control of autonomous underwater vehicle (AUV) in heading and depth attitude via self-adaptive fuzzy PID controller," *J. Marine Sci. Technol.*, vol. 20, no. 3, pp. 559–578, 2015.
- [14] J. Xu, M. Wang, and L. Qiao, "Backstepping-based controller for three-dimensional trajectory tracking of underactuated unmanned underwater vehicles," *Control Theory Appl.*, vol. 31, no. 11, pp. 1589–1596, 2014.
- [15] X. Xiang, C. Yu, and Q. Zhang, "Robust fuzzy 3D path following for autonomous underwater vehicle subject to uncertainties," *Comput. Oper. Res.*, vol. 84, pp. 165–177, 2016.
- [16] A. Chemori, K. Kuusmik, T. Salume, and M. Kruusmaa, "Depth control of the biomimetic U-CAT turtle-like AUV with experiments in real operating conditions," in *Proc. IEEE Int. Conf. Robot. Autom.*, Stockholm, Sweden, May 2016, pp. 4750–4755.
- [17] G. V. Lakhekar and R. G. Roy, "Heading control of an underwater vehicle using dynamic fuzzy sliding mode controller," in *Proc. Int. Conf. Circuits, Power, Comput. Technol.*, Nagercoil, India, Mar. 2014, pp. 1448–1454.
- [18] R. Cui, X. Zhang, and D. Cui, "Adaptive sliding-mode attitude control for autonomous underwater vehicles with input nonlinearities," *Ocean Eng.*, vol. 123, pp. 45–54, 2016.
- [19] Z. Yan, H. Ju, and S. Hou, "Diving control of underactuated unmanned undersea vehicle using integral-fast terminal sliding mode control," *J. Central South Univ.*, vol. 23, no. 5, pp. 1085–1094, 2016.
- [20] H. Zhou, K. Liu, Y. Li, and S. Ren, "Dynamic sliding mode control based on multi-model switching laws for the depth control of an autonomous underwater vehicle," *Int. J. Adv. Robot. Syst.*, vol. 12, no. 7, pp. 1–10, 2015, doi: <https://doi.org/10.5772/61038>.
- [21] T. Elmokadem, M. Zribi, and K. Youcef-Toumi, "Trajectory tracking sliding mode control of underactuated AUVs," *Nonlinear Dyn.*, vol. 84, no. 2, pp. 1079–1091, 2016.
- [22] J. Yu, F. Sun, D. Xu, and M. Tan, "Embedded vision-guided 3-D tracking control for robotic fish," *IEEE Trans. Ind. Electron.*, vol. 63, no. 1, pp. 355–363, Jan. 2016.
- [23] G. V. Lakhekar and V. D. Saundarmal, "Novel adaptive fuzzy sliding mode controller for depth control of an underwater vehicles," in *Proc. Int. Conf. Fuzzy Syst.*, Hyderabad, India, Aug. 2013, pp. 1–7.
- [24] S. Pezeshki, A. R. Ghiasi, M. A. Badamchizadeh, and K. Sabahi, "Adaptive robust control of autonomous underwater vehicle," *J. Cont., Autom. Elect. Syst.*, vol. 27, no. 3, pp. 250–262, 2016.
- [25] J. Yu, S. Chen, Z. Wu, and W. Wang, "On a miniature free-swimming robotic fish with multiple sensors," *Int. J. Adv. Robot. Syst.*, vol. 13, no. 62, pp. 1–8, 2016, doi: <https://doi.org/10.5772/62887>.

- [26] J. Yu, Z. Su, M. Wang, M. Tan, and J. Zhang, "Control of yaw and pitch maneuvers of a multilink dolphin robot," *IEEE Trans. Robot.*, vol. 28, no. 2, pp. 318–329, Apr. 2012.
- [27] J. Liu, Z. Wu, and J. Yu, "Design and implementation of a robotic dolphin for water quality monitoring," in *Proc. IEEE Int. Conf. Robot. Biomimetics*, Qingdao, China, Aug. 2016, pp. 835–840.
- [28] Z. Wu, J. Liu, J. Yu, and F. Hao, "Development of a novel robotic dolphin and its application to water quality monitoring," *IEEE/ASME Trans. Mechatronics*, to be published.
- [29] X. Chen and J. Li, "AUV planner tracking control based on the line of sight guidance method," in *Proc. IEEE Int. Conf. Mechatronics Autom.*, Tianjin, China, Aug. 2014, pp. 1204–1208.
- [30] R. Yu, Q. Zhu, G. Xia, and Z. Liu, "Sliding mode tracking control of an underactuated surface vessel," *IET Control Theory Appl.*, vol. 6, no. 3, pp. 461–466, 2012.
- [31] W. Chen, Y. Wei, H. Liu, and H. Zhang, "Bio-inspired sliding mode controller for ROV with disturbance observer," in *Proc. IEEE Int. Conf. Mechatronics Autom.*, Harbin, China, Aug. 2016, pp. 599–604.
- [32] J. Li, M. Kong, X. Chen, and L. Li, "AUV control systems of nonlinear extended state observer design," in *Proc. IEEE Int. Conf. Mechatronics Autom.*, Tianjin, China, Aug. 2014, pp. 1924–1928.
- [33] A. T. Azar and Q. Zhu, *Advances and Applications in Sliding Mode Control Systems* (Volume 576 of Studies in Computational Intelligence). Berlin, Germany: Springer, 2015.
- [34] J. Ghommam, F. Mnif, and N. Derbel, "Global stabilisation and tracking control of underactuated surface vessels," *IET Control Theory Appl.*, vol. 4, no. 1, pp. 71–88, 2010.
- [35] M. Wang, J. Yu, M. Tan, D. Wang, and C. Li, "CPG-based multi-modal swimming control for robotic dolphin," *Acta Automat. Sin.*, vol. 40, no. 9, pp. 1933–1941, 2014.



Jincun Liu received the B.E. degree in electronic and information engineering and the M.E. degree in control theory and control engineering from the School of Information and Electrical Engineering, Shandong Jianzhu University, Jinan, China, in 2011 and 2014, respectively. He is currently working toward the Ph.D. degree in control theory and control engineering in the State Key Laboratory of Management and Control for Complex Systems, Institute of Automation, Chinese Academy of Sciences, Beijing, China.

He is currently with the University of Chinese Academy of Sciences, Beijing, China. His current research interests include intelligent control of bioinspired underwater robots.



Zhengxing Wu received the B.E. degree in logistics engineering from the School of Control Science and Engineering, Shandong University, Jinan, China, in 2008, and the Ph.D. degree in control theory and control engineering from the Institute of Automation, Chinese Academy of Sciences (IACAS), Beijing, China, in 2015.

He is currently an Assistant Professor in the State Key Laboratory of Management and Control for Complex Systems, IACAS. His research interests include fast maneuvers of bioinspired

robotic fish and gliding motions of robotic dolphins.



Junzhi Yu (SM'14) received the B.E. degree in safety engineering and the M.E. degree in precision instruments and mechatronics from the North University of China, Taiyuan, China, in 1998 and 2001, respectively, and the Ph.D. degree in control theory and control engineering from the Institute of Automation, Chinese Academy of Sciences (IACAS), Beijing, China, in 2004.

He is currently a Professor in the State Key Laboratory of Management and Control for Complex Systems, IACAS. His research interests include biomimetic robots, intelligent control, and intelligent mechatronic systems.

Dr. Yu is as an Associate Editor of the IEEE TRANSACTIONS ON ROBOTICS and the IEEE/ASME TRANSACTIONS ON MECHATRONICS.



Hao Fang received the B.S. degree from the Xi'an University of Technology, Xi'an, China, in 1995, and the M.S. and Ph.D. degrees in control science and engineering from Xi'an Jiaotong University, Xi'an, China, in 1998 and 2002, respectively.

He held two postdoctoral appointments in the French Institute for Research in Computer Science and Automation, Blaise Pascal University, Clermont-Ferrand, France. Since 2011, he has been a Professor in the Beijing Institute of Technology, Beijing, China. His current research interests include robotic control, mobile robots, and parallel manipulators.